



HAL
open science

Development of viable TAP-tagged dengue virus for investigation of host–virus interactions in viral replication

Teera Poyomtip, Kenneth Hodge, Ponpan Matangkasombut, Anavaj Sakuntabhai, Trairak Pisitkun, Siwanon Jirawatnotai, Sarin Chimnaronk

► To cite this version:

Teera Poyomtip, Kenneth Hodge, Ponpan Matangkasombut, Anavaj Sakuntabhai, Trairak Pisitkun, et al.. Development of viable TAP-tagged dengue virus for investigation of host–virus interactions in viral replication. *Journal of General Virology*, 2016, 97 (3), pp.646-658. 10.1099/jgv.0.000371 . pasteur-02082706

HAL Id: pasteur-02082706

<https://pasteur.hal.science/pasteur-02082706>

Submitted on 3 Apr 2019

HAL is a multi-disciplinary open access archive for the deposit and dissemination of scientific research documents, whether they are published or not. The documents may come from teaching and research institutions in France or abroad, or from public or private research centers.

L'archive ouverte pluridisciplinaire **HAL**, est destinée au dépôt et à la diffusion de documents scientifiques de niveau recherche, publiés ou non, émanant des établissements d'enseignement et de recherche français ou étrangers, des laboratoires publics ou privés.

Development of viable TAP-tagged dengue virus for investigation of host–virus interactions in viral replication

Teera Poyomtip,^{1†} Kenneth Hodge,^{2†} Ponpan Matangkasombut,^{1,3} Anavaj Sakuntabhai,^{3,4,5} Trairak Pisitkun,⁶ Siwanon Jirawatnotai^{3,7} and Sarin Chimnaronk^{2,3}

Correspondence

Siwanon Jirawatnotai
siwanon.jir@mahidol.ac.th
Sarin Chimnaronk
sarin.chi@mahidol.ac.th

¹Department of Microbiology, Faculty of Science, Mahidol University, Bangkok 10400, Thailand

²Institute of Molecular Biosciences, Mahidol University, Salaya Campus, Phutthamonthon, Nakhon Pathom 73170, Thailand

³Systems Biology of Diseases Research Unit, Faculty of Science, Mahidol University, Bangkok 10400, Thailand

⁴Functional Genetics of Infectious Diseases Unit, Institute Pasteur, Paris, France

⁵Centre National de la Recherche Scientifique (CNRS), URA3012, F-75015 Paris, France

⁶Systems Biology Center, Faculty of Medicine, Chulalongkorn University, Bangkok 10330, Thailand

⁷Department of Pharmacology, Faculty of Medicine, Siriraj Hospital, Mahidol University, Bangkok 10700, Thailand

Dengue virus (DENV) is a mosquito-borne flavivirus responsible for life-threatening dengue haemorrhagic fever (DHF) and dengue shock syndrome (DSS). The viral replication machinery containing the core non-structural protein 5 (NS5) is implicated in severe dengue symptoms but molecular details remain obscure. To date, studies seeking to catalogue and characterize interaction networks between viral NS5 and host proteins have been limited to the yeast two-hybrid system, computational prediction and co-immunoprecipitation (IP) of ectopically expressed NS5. However, these traditional approaches do not reproduce a natural course of infection in which a number of DENV NS proteins colocalize and tightly associate during the replication process. Here, we demonstrate the development of a recombinant DENV that harbours a TAP tag in NS5 to study host–virus interactions *in vivo*. We show that our engineered DENV was infective in several human cell lines and that the tags were stable over multiple viral passages, suggesting negligible structural and functional disturbance of NS5. We further provide proof-of-concept for the use of rationally tagged virus by revealing a high confidence NS5 interaction network in human hepatic cells. Our analysis uncovered previously unrecognized hnRNP complexes and several low-abundance fatty acid metabolism genes, which have been implicated in the viral life cycle. This study sets a new standard for investigation of host–flavivirus interactions.

Received 16 November 2015

Accepted 11 December 2015

INTRODUCTION

Dengue virus (DENV), Japanese encephalitis virus, West Nile virus and yellow fever virus are flaviviruses of well-publicized epidemiological importance. Of these, DENV is the world's most common arthropod-borne virus, afflicting approximately 390 million individuals per year (Bhatt *et al.*, 2013). DENV is most prevalent in tropical and subtropical regions such as South and SouthEast Asia,

the Western Pacific and Central and South America. Advances in biotechnology have thus far failed to stem a net increase in infections over the past 50 years; the World Health Organization reported that from 1955 to 2007, the number of DENV-infected patients increased over 1000-fold (WHO, 2009). DENV causes a wide range of diseases in humans, from a self-limiting dengue fever to a life-threatening syndrome called dengue haemorrhagic fever (DHF) or dengue shock syndrome (DSS). No vaccines or drugs are currently approved for therapeutic treatment.

The genome of DENV is an approximately 10.7 kb positive ssRNA that is composed of a long ORF of a viral

†These authors contributed equally to this work.

Three supplementary tables are available with the online Supplementary Material.

polyprotein of 3390 amino acids. The polyprotein is proteolytically processed into three structural proteins (C, prM and E) and seven non-structural (NS) proteins (NS1, NS2A, NS2B, NS3, NS4A, NS4B and NS5) at the endoplasmic reticulum (ER) membrane. Among viral proteins, NS5 is the largest protein, possessing methyltransferase (MTase) and RNA-dependent RNA polymerase (RdRp) activities in its N- and C-termini, responsible for capping the 5' end and generation of new genomic viral RNA in infected cells, respectively (Dong *et al.*, 2014). NS5 recruits at least NS3 and a subset of host cellular proteins to form the replication complex or 'replicase' in virus-induced membranous compartments for productive viral RNA synthesis (Bidet & Garcia-Blanco, 2014). NS5 also plays important roles as an immune suppressor by downregulating type I IFN responses through interacting with STAT2 (Ashour *et al.*, 2009). Moreover, both NS3 and NS5 were implicated in DHF as they were found to be the immunodominant T-cell antigens compared to other viral proteins (Duangchinda *et al.*, 2010). Hence, NS5 has long been considered an attractive drug target due to its multiple crucial roles in viral replication (Dong *et al.*, 2008), and its cellular interaction partners may also reveal new therapeutic avenues for fatal DHF or DSS (Krishnan & Garcia-Blanco, 2014).

A number of approaches have been used to identify NS5-interacting partners (Carpp *et al.*, 2014; Doolittle & Gomez, 2011; Khadka *et al.*, 2011; Le Breton *et al.*, 2011; Mairiang *et al.*, 2013). The yeast two-hybrid system (Y2H) offers the advantage of rapid large-scale screening of protein pairs. However, the method usually does not take into account both cellular localization and abundance of particular interactions in specific cell types. Flaviviral Y2H studies conducted by different groups have, thus far, shown a curious lack of overlap in their datasets. For example, Khadka *et al.* (2011) and Le Breton *et al.* (2011) both generated DENV NS5 interaction networks, with no overlapping data (Krishnan & Garcia-Blanco, 2014).

Affinity isolation of ectopically expressed viral proteins is another approach to analyse the host–virus interactome, which frequently renders extensive lists of interactors. However, overexpression of NS5 alone should not mimic physiological conditions (Rigaut *et al.*, 1999). Such an approach downplays a body of work that suggests that viral RNA and proteins are tightly associated from translation to later stages in the viral life cycle; for example, ectopically expressed NS5 was not able to complement viruses carrying various NS5 mutants (Khromykh *et al.*, 1999). Presumably, the introduced NS5 failed to insinuate itself into existing viral replicases which, depending on the stage of infection, might be protected by membranous compartments in the ER (Welsch *et al.*, 2009). Recent work with tobacco mosaic virus has demonstrated a tight association between its RdRp and genome from the time of translation through replication (Kawamura-Nagaya *et al.*, 2014). The limitations of ectopic expression have also been reported with the other replicase component

NS3, showing that the inability of introduced WT NS3 to overcome the deficiencies of mutant viral NS3 could be observed at the assembly stage of the viral life cycle (Liu *et al.*, 2002).

To eliminate or minimize the aforementioned deficiencies, immunoprecipitation (IP) of NS5 polymerase from infected cells via an anti-NS5 antibody could be achieved; however, acquisition of a monoclonal antibody that recognizes epitopes in a native form of protein with high specificity and affinity is a key bottleneck and challenge. A viable recombinant virus with a tagged NS5 polymerase would be ideal for investigation of its interacting partners. Moreover, the endogenous tag would permit studies of the cellular localization of NS5 and its partners, as well as the timing of NS5-related events in the viral life cycle, with physiological relevance. In this study, we demonstrate, to our knowledge for the first time, a rational design of infectious DENV carrying a tandem affinity purification (TAP) tag inside NS5, allowing the identification of a landscape of NS5-interacting proteins in infected hepatic cells, a natural target of DENV.

RESULTS

Design and production of recombinant NS5-tagged DENV

A previous study attempting to incorporate a tag into NS5 in viable DENV was unsuccessful (Carpp *et al.*, 2014). Initially, we attempted to generate an infectious recombinant DENV carrying a tag following the NS5 polyprotein cleavage site (GTGNIG) immediately downstream of the N-terminus, and a tag at the C-terminus of NS5. However, tags at these locations completely disabled viral replication and propagation. Therefore, we selected a more rational approach to seek possible tag locations. NS5 sequences from ten flaviviruses were aligned and scored. In our scheme, there were seven regions at which a conservation value, calculated over 31 residue windows, was obviously low (Fig. 1a). These regions were then mapped onto the crystal structure of DENV NS5 to winnow out insert sites that could interfere with structures (i.e. α -helices or β -sheets) or that would be located inside the protein core. A final screening procedure examined potential insert sites for the presence of eukaryotic linear motifs that might be of importance (Dinkel *et al.*, 2012). Finally, the positions of interest were required to have a minimum 10 Å distance from the two active sites (MTase and RdRp) of NS5. Combining the above criteria, we identified suitable regions at N172–N177 of the MTase domain and Q633–T636 of the RdRp domain. The TAP tag containing a poly-histidine (eight amino acids) and FLAG (eight amino acids) tags, which facilitate a two-step protein purification and reduce non-specific background, was inserted following N173 in MTase or T636 in DENV-2 RdRp (Fig. 1b). We also placed a glycine linker between the

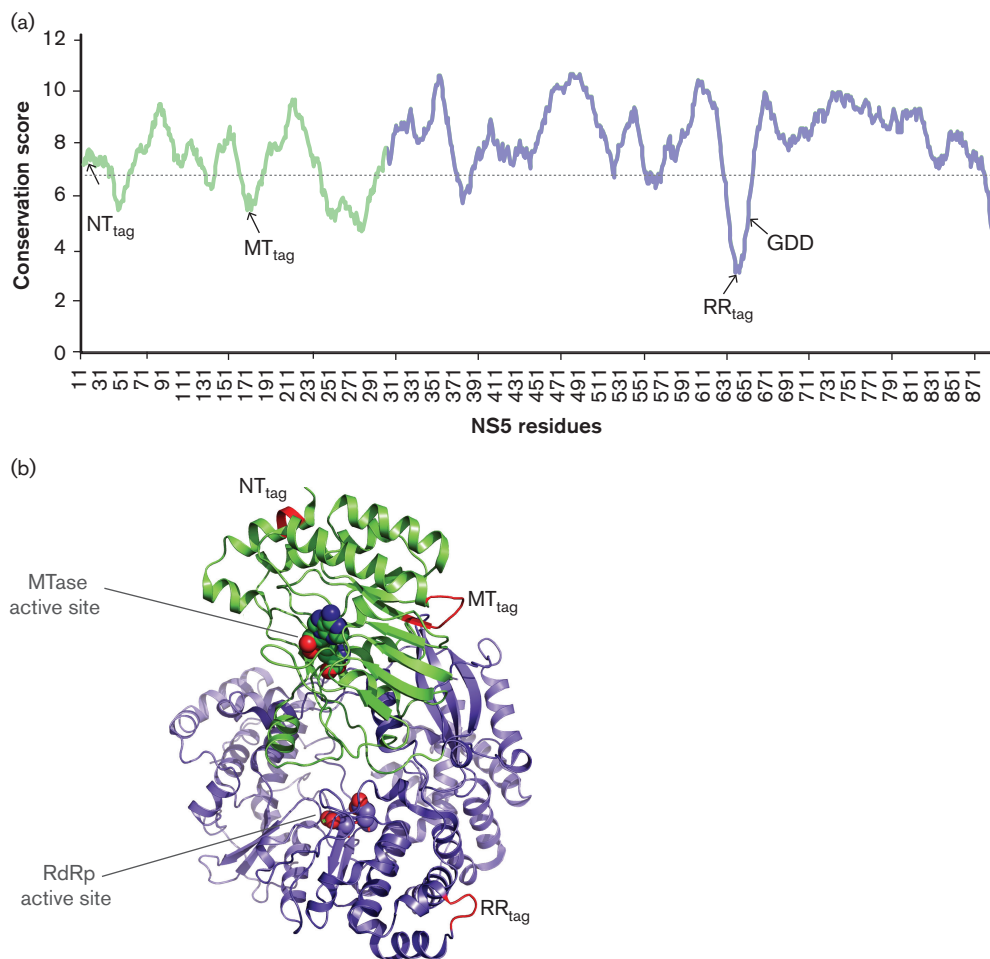


Fig. 1. Rational design for tagging DENV NS5. (a) Analysis of amino acid conservation among 11 flaviviral NS5s. Means of summed CLUSTAL Omega conservation scores over all 31 amino acid frames are plotted against NS5 residues including MTase (green) and RdRp (blue) domains. The dotted line is positioned one SD unit (1.23) below the mean conservation value (7.95); note the seven troughs below this cut-off. (b) DENV-3 NS5 crystal structure. Red colour represents the insertion position of the TAP tag. The polymerase active site is indicated by the GDD catalytic triad.

poly-histidine and FLAG epitopes to increase their flexibility and accessibility (Sabourin *et al.*, 2007).

The full-length DENV-2 RNA genome with tagged NS5 (10.7 kb) was synthesized *in vitro* using T7 RNA polymerase (Fig. 2a). DENV transcripts from pD2-IC (WT) and three recombinant constructs each carrying the TAP tag at the N-terminus of NS5 (NT_{tag}), inside MTase (MT_{tag}) or in RdRp (RR_{tag}), were transfected into BHK-21 cells, and their effects on viral production inside the cells were investigated at 2, 4 and 7 days post-infection via immunofluorescence signals of DENV E protein. Only the MT_{tag} construct showed E protein expression in a time-dependent manner similar to that of WT, whereas the NT_{tag} and RR_{tag} rendered negative results (Fig. 2b) similarly to our earlier C-terminally tagged NS5 construct (data not shown). Our results indicated that understanding of the protein sequence and structure is essential for success in insertion

of an extra sequence into the compact viral genome, and our rational approach should be useful for tag insertion into other viral proteins.

Next, we examined the production of infectious DENV from our NS5-tagged constructs. The foci formation assays were performed with supernatants obtained 7 days post RNA transfection into BHK-21 cells. The results were consistent with the E protein expression profiles, revealing that the MT_{tag} clone could produce infectious viral particles comparable to the WT clone from pD2-IC (Fig. 2c). We also generated an MT_{tag} construct that possessed an alternative HA-FLAG tag epitope in the same position, and this tagged version also gave infectious particles (data not shown). Therefore, the N172–N177 loop of MTase is a suitable location, with the tag having a minimal effect on viral replication and production, for general tag insertion into flaviviral NS5s.

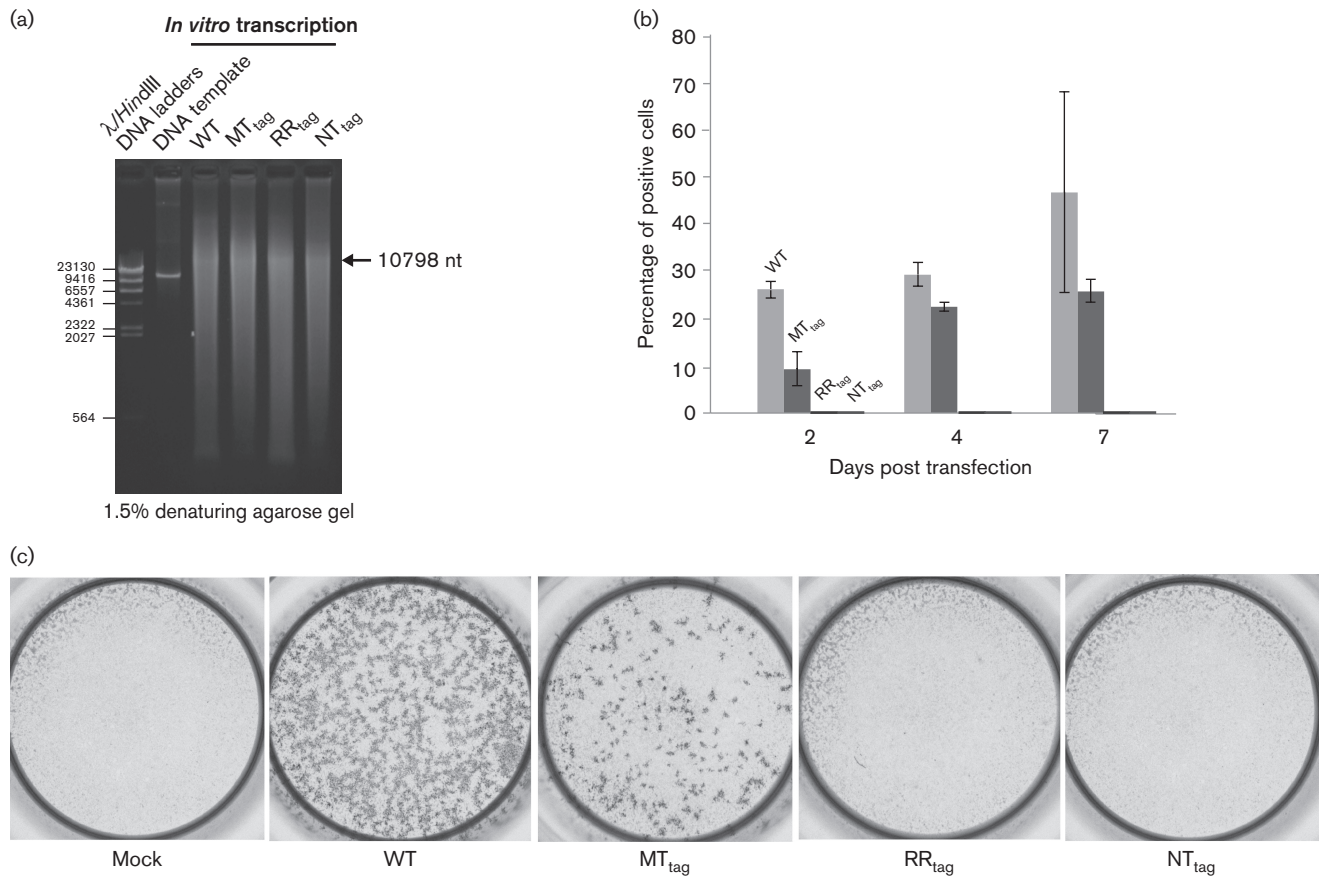


Fig. 2. Screening of various tagged DENV constructs. (a) Formamide gel electrophoresis shows the quality of *in vitro* transcribed products. Arrow shows the size of the full-length DENV genome. (b) DENV transcripts were electroporated into BHK-21 cells and the synthesis of E protein in transfected cells was measured via immunofluorescence. Light and dark grey bars represent WT and MT_{tag} transfections, respectively. Blank spaces highlight the absence of detected E protein in RR_{tag} and NT_{tag} constructs. Hereafter, the graphs show means of experiments performed in triplicate, and the error bars show SD. (c) Representative data from two independent experiments show focus forming assays of culture media from RNA-transfected cells at day 7.

Characterization of MTase-tagged DENV

We collected supernatants obtained at 7 days post RNA transfection and increased the viral titre by another three passages in BHK-21. Then, engineered tagged DENV particles recovered from the MT_{tag} construct (hereafter designated etDENV) were used to infect BHK-21 at an m.o.i. of 1 and 0.01 for observation of phenotype and viral kinetics, respectively. Our etDENV induced rounded cell shapes which represent a cytopathic effect in cell culture at day 2 post-infection similar to the natural DENV-2 strain 16681 (Fig. 3a). Production of infectious etDENV showed an identical pattern to those of DENV-2 from natural strain 16681 and virions derived from supernatant of RNA-transfected cells (WT), reaching peaks of viral titre of approximately 10^6 FFU ml⁻¹ at day 4 (Fig. 3b). Besides BHK-21 cells, flow cytometry analysis showed that our etDENV also possessed infectivity in A549, HEK-293 and Huh-7 cell lines, representing virus targeting of human

lung, kidney and liver, respectively. However, the infectivity is about 60 % of that of WT (Fig. 3c).

Next, we confirmed that the tags would not interfere with the localization of NS5 between nucleus and cytoplasm that has been demonstrated for DENV serotypes 2 and 4 (Hannemann *et al.*, 2013). At day 2 post-infection in BHK-21 cells at an m.o.i. of 1, NS5s of both WT and etDENV mainly localized in the nucleus as described earlier (Uchil *et al.*, 2006) (Fig. 3d). Finally, we validated the stability of the tag in etDENV, since the possibility that the virus could remove or modify the epitope tag after several passages has been proposed (Schoggins *et al.*, 2012; Usme-Ciro *et al.*, 2014). The etDENV collected after seven passages in BHK-21 was sequenced (Fig. 3e). No mutation or deletion was found around the insertion region, indicating a high stability of these insertion clones. These results also suggested that the tag insertion did not disturb the folding and function of NS5 in infected cells. Taken together, our etDENV showed

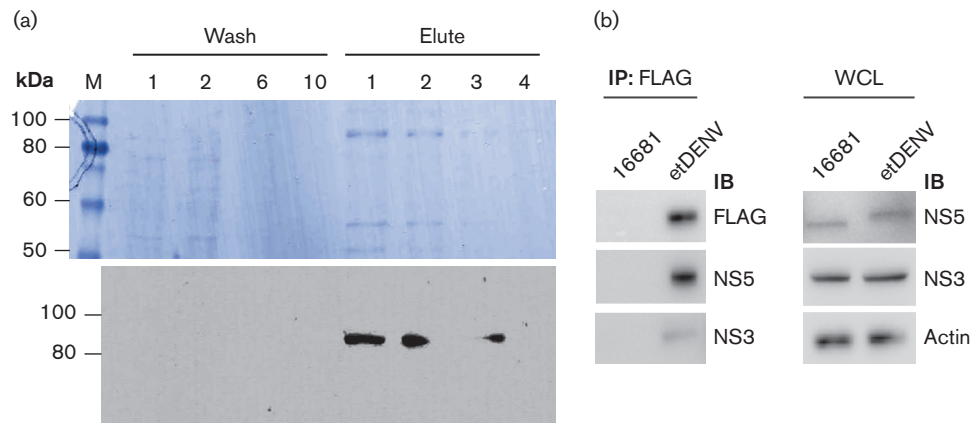


Fig. 4. Purification of NS5 via the internal TAP tag. (a) Ni affinity purified fractions were analysed by SDS-PAGE (top panel) and immunoblotting (IB) (lower panel). Wash and elution fractions are indicated above the lanes. (b) FLAG IP fractions were subjected to IB with specific antibodies. WCL, Whole cell lysate.

identical properties to WT DENV-2, and is suitable for studying the NS5 interactome in different cell types. To our knowledge, this is the first report of stable, infectious recombinant NS5-tagged flavivirus.

Isolation of tagged NS5 from infected cells

Since the TAP tag existed inside the MTase domain, we validated its ability to isolate NS5-interacting complexes via both His and FLAG tag pull downs. For Ni affinity, we infected Huh-7 cells with etDENV at an m.o.i. of 5, and extracted the total protein 48 h after infection. After Ni affinity purification, the results showed clear NS5 bands in both SDS-PAGE and Western blot analyses, suggesting that this internal tag was exposed to the solvent and useful for isolation (Fig. 4a). Based on purified recombinant DENV RdRp as standards in Western blot analysis (Kamkaew & Chimnaroon, 2015), we calculated the total amount of NS5 as approximately 500 ng from 10^7 cells; therefore, giving 9.4×10^5 NS5 molecules (infected cell)⁻¹ (a molecular mass of 1.06×10^5 Da or 1.76×10^{-19} g). Furthermore, we also performed IP of NS5 via the FLAG tag from BHK-21 cells which were infected at an m.o.i. of 1. As with Ni affinity, the IP with a FLAG antibody was highly effective in pulling down NS5 with a very low background (Fig. 4b). NS3, a well-known NS5 interactor, was detected in the co-IP fraction of etDENV. Taken together, we have here provided a new biological tool for studying host-DENV interactions.

Interactome of DENV NS5 in human liver cells

To explore an interaction landscape of NS5 in liver cells, Huh-7 cells were infected with either etDENV or DENV-2 16681 at an m.o.i. of 5, and the NS5 complexes were isolated via FLAG IP at 48 h post-infection followed by mass spectrometry. Only DENV NS5 interactors that

were found in etDENV IP samples, but not in the control, were considered. Moreover, we utilized two distinct algorithms for peptide identification, and only 97 proteins overlapping between 554 X! Tandem and 199 SEQUEST candidates were considered, and mapped by STRING 10.0 software (Table S2). To reveal a high-confidence interactome, this network was reconstructed to include two forms of information (Fig. 5a). First, STRING's protein-protein interaction confidence levels were shown as edge widths. Secondly, relative peptide abundances from mass spectrometry were indicated by node sizes. In addition to the host proteins, the NS3 helicase was identified, confirming its role as the major viral protein interacting with NS5 (Table 1). Our NS5 interaction network contained only four proteins that were also reported as NS5 interactors in recent genome-wide studies (Table 2). Intriguingly, heterogeneous nuclear ribonucleoproteins (hnRNPs) were identified as the main NS5 complex for the first time. Several NS5 interactors related to the protein-folding pathway have already been shown to be upregulated upon DENV infection (Fig. 5a and Table 3). Though our interactome map was constructed with proteins found only in the etDENV IP, we did examine the control-only protein list for possible insights. However, none of the predicted functional control-only groups reached the significance of the top 15 etDENV IP groups, with one exception (enrichment in desmosome-related proteins in the control group). Further, comparing the top 15 enriched groups derived from etDENV and control IP, no overlap was observed, with enriched groups from control IP focusing on cell-junction related functions (e.g. 'anchoring junction', 'desmosome' and 'cell-cell junction'), whereas cytosol and RNA-binding functions dominated in the etDENV IP (Fig. 5b and Table S3). The clear difference in the contents of control versus etDENV pulldowns again points to the efficacy of etDENV in isolating NS5-specific interactors.

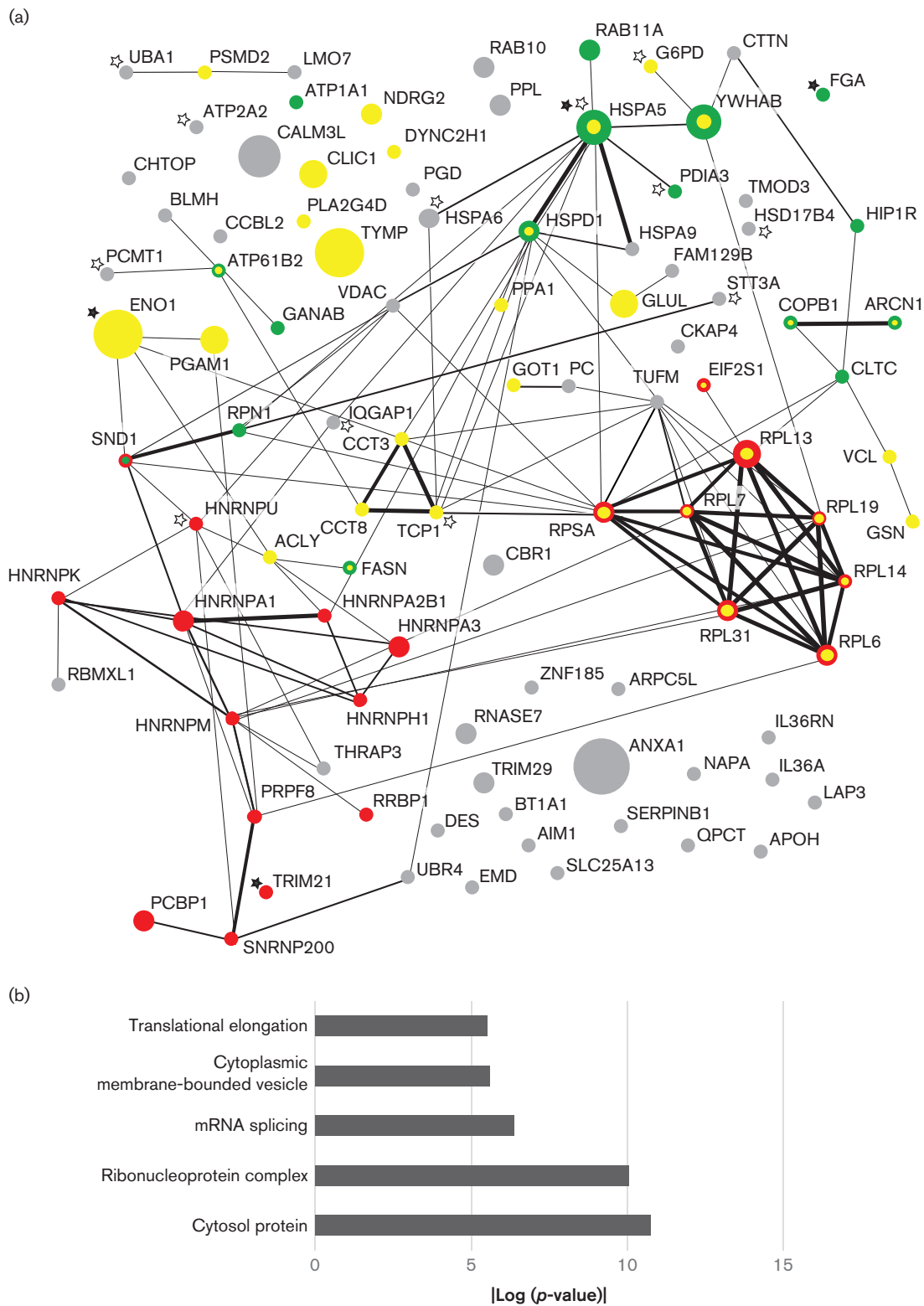


Fig. 5. NS5 interactome in Huh-7 cells. (a) The protein–protein interaction network was reconstructed using the initial STRING 10.0 network as template. Colours indicate three enriched groups: yellow for non-membranous predominantly cytosolic proteins, red for ribonucleoproteins and green for cytoplasmic membrane-bound vesicle proteins. Open and filled stars indicate proteins with altered expression levels and NS5 interactors identified in previous studies, respectively (Table 3). Edge length and node placement are not of importance. Isolated nodes should not be construed as irrelevant to infection. (b) List of enriched gene ontology groups using DAVID.

Table 1. DENV proteins identified by NS5 IP

| Viral protein | Peptides | Molecular mass (kDa) |
|---------------|----------|----------------------|
| prM | 1 | 18.92 |
| NS1 | 1 | 39.93 |
| NS3 | 10 | 69.26 |
| NS4A | 1 | 13.96 |
| NS5 | 24 | 103.2 |

DISCUSSION

In the early stages of our work, we unsuccessfully attempted to place epitope tags into the N- and C-termini of several DENV proteins. The vast majority of TAP-tag experiments have placed the tag at a protein's N- or C-terminus. Generally, such an approach should offer minimal disruption of the protein structure and function. Carpp *et al.* (2014) also pointed out an inability to insert tags into DENV NS3 and NS5 proteins in the context of viable virus, and their subsequent work, therefore, depended on ectopic expression. On the other hand, Teterina *et al.* (2011) used a transposon-based method to

randomly insert 15 nt sequences into the poliovirus genome. Viable viruses were then found to contain tags predominantly within regions of low conservation and at surface-exposed loops. These results were later successfully applied to specifically tag foot-and-mouth disease virus protein 3a (Li *et al.*, 2012). This work highlighted the potential for a rational tagging strategy based on both sequence conservation and tertiary structure.

Our success in tag insertion within NS5's MTase indicated that internal insertions may be underrated in their utility. In the context of a viral genome, such tags are particularly useful, as terminal insertions may interfere with polyprotein processing. At the same time, virus with a rationally designed internal RdRp tag was not viable, highlighting the still unpredictable effects of tag insertion. One simple factor that may have contributed to our final success, however, would be the size of the tags, with $8 \times$ His and FLAG combo contributing less than 25 residues to NS5. Previous work has established that insert size and type certainly could be a factor in viral viability; in one case, a relatively large luciferase insert within WNV capsid was quickly eliminated over passaging, while a 75 nt portion of a TAT insert (from HIV) remained stable over multiple

Table 2. NS5 interactors identified in this study and other earlier reports

| Gene ID | Symbol | Methodology | Function(s) | Reference |
|-----------------|--------|-------------|---|--------------------------------|
| ENSG00000044574 | HSPA5 | Y2H | Protein folding and protein assembly | Mairiang <i>et al.</i> (2013) |
| ENSG00000074800 | ENO1 | Y2H | Glycolysis enzyme and tumour suppressor | Le Breton <i>et al.</i> (2011) |
| ENSG00000132109 | TRIM21 | Y2H | Protein degradation process | Le Breton <i>et al.</i> (2011) |
| ENSG00000171560 | FGA | Y2H | Blood coagulation | Khadka <i>et al.</i> (2011) |

Table 3. Identified NS5 interactors that showed alteration of gene expression upon DENV infection

| Gene ID | Symbol | Expression | Function(s) | Reference(s) |
|-----------------|---------|--------------------------------|---|--|
| ENSG00000044574 | HSPA5 | Upregulation in Huh-7 and A549 | Folding and protein assembly | Chiu <i>et al.</i> (2014); Pando-Robles <i>et al.</i> (2014) |
| ENSG00000120265 | PCMT1 | Downregulation in ECV | Type II carboxyl methyltransferase enzyme | Liew & Chow (2006) |
| ENSG00000120438 | TCP1 | Upregulation in Huh-7 | Chaperone protein | Pando-Robles <i>et al.</i> (2014) |
| ENSG00000130985 | UBA1 | Upregulation in Huh-7 | Protein degradation process | Pando-Robles <i>et al.</i> (2014) |
| ENSG00000133835 | HSD17B4 | Upregulation in A549 | Peroxisomal β -oxidation | Chiu <i>et al.</i> (2014) |
| ENSG00000134910 | STT3A | Upregulation in A549 | N-Oligosaccharyltransferase complex | Chiu <i>et al.</i> (2014) |
| ENSG00000140575 | IQGAP1 | Upregulation in Huh-7 | Reorganization of cytoskeleton process | Pando-Robles <i>et al.</i> (2014) |
| ENSG00000153187 | HNRNPU | Upregulation in Huh-7 | mRNA processing | Pando-Robles <i>et al.</i> (2014) |
| ENSG00000160211 | G6PD | Upregulation in Huh-7 | Energy generation | Pando-Robles <i>et al.</i> (2014) |
| ENSG00000167004 | PDIA3 | Upregulation in A549 and HepG2 | Folding and disulfide isomerase enzyme | Chiu <i>et al.</i> (2014); Higa <i>et al.</i> (2008) |
| ENSG00000174437 | ATP2A2 | Upregulation in A549 | Hydrolysis of ATP in ER | Chiu <i>et al.</i> (2014) |
| ENSG00000173110 | HSPA6 | Upregulation in HepG2 | Protein folding | Fink <i>et al.</i> (2007) |

passages (Vandergaast *et al.*, 2014). Similarly, a C-terminal GFP tag of Sindbis virus's RdRp failed to infect cells, but virus was viable when the tag was switched to $3 \times$ FLAG (Cristea *et al.*, 2010). Yet another study showed that insertion of the smaller luciferase gene into the dengue genome rendered more stable recombinant virus, while the epitope was lost over a series of passages when the GFP gene was exploited instead (Schoggins *et al.*, 2012; Usme-Ciro *et al.*, 2014). The luciferase gene could also be successfully inserted into the N-terminal region of the capsid in DENV genome despite possible concerns that it would disrupt viral packaging (Zou *et al.*, 2011).

DENV infects several organs in humans, altering host homeostasis and counteracting the host response (Aye *et al.*, 2014; Póvoa *et al.*, 2014). These events suggest complex interactions between host and virus where viral proteins play roles in several networks. However, current systems for studying the host–DENV interaction network may not be up to the task of emulating actual infection conditions. By placing a tag sequence within an organism's genome, the protein in question can be expressed, localized and regulated under natural infection conditions and, at the same time, isolated along with its protein partners with high specificity.

Our functional annotation showed highest enrichment in cytosolic proteins, a category that excluded membranous and subcellular components. Enrichment in cytosolic membranous components was also high, consistent with NS5's localization with the ER during replication. RNPs were abundant within the interactor list, with a subset of splicing-related hnRNPs (hnRNPM, hnRNPA1, hnRNPA3, hnRNPU, hnRNPK, hnRNPH1 and hnRNPA2B1), which are generally localized to the nucleus, showing particular enrichment. Earlier work suggested that DENV genomic RNA lacks splicing sites (Brunak *et al.*, 1991), although one study predicted a candidate donor splicing present on the DENV genome (Usme-Ciro *et al.*, 2014). Interestingly, a previous study examining the infected Huh-7 proteome showed significant alterations in the abundance of RNA processing proteins (Pando-Robles *et al.*, 2014). While DENV-2 NS5 could shuttle between the nucleus and cytoplasm, and thus hnRNPs might not be necessarily associated with the replication complex, it has been revealed that the hnRNPK and hnRNPA1 proteins accumulated in the cytoplasm and promoted DENV production (Anwar *et al.*, 2009; Brunetti *et al.*, 2015; Jiang *et al.*, 2009). However, precise roles played by interaction of hnRNPs with NS5 require further study. Another subset of RNP interactors was related to the translational elongation process. In particular, large ribosomal subunit members (RPL6, RPL7, RPL13, RPL14, RPL19 and RPL31) were identified as NS5 interaction partners, with only low levels of other ribosome proteins found in the control group. Though translational elongation and viral replication are processes that, logically, cannot occur simultaneously, Germain *et al.* (2014) also found ribosomal proteins interacting with the HCV polymerase.

Conceivably, the NS5–ribosome interaction might enhance and/or inhibit translation according to a need for protein versus RNA, without any conflicts between translation and replication.

We also divided the number of fragments detected by molecular mass and abundance (in p.p.m. of protein) in the liver (PaxDb version 4.0) to reduce bias towards abundant proteins (Wang *et al.*, 2015). The phospholipase 2 protein (PLA2G4D) came to the fore. Since it was shown that phospholipase 2 group 4C was involved in generation of the membranous web in HCV-infected cells (Xu *et al.*, 2012), PLA2G4D could play a similar role in remodelling the ER membrane for DENV replication. In concord with this picture, fatty acid synthase (FASN), which was shown to be relocalized to viral replicase to remodel cytosolic membranes in DENV-infected cells (Heaton *et al.*, 2010), was also present in our interactome map. Other interactors involved in lipid metabolism included pyruvate carboxylase (PC), ATP citrate lyase (ACLY) and butyrophilin (BT1A1). Our results suggest tight association of fatty acid biosynthesis complex with viral replicase.

It might be informative to compare our interactome with that of Carpp *et al.* (2014), in which DENV-2 NS5 was ectopically expressed in infected cells as a C-terminally GFP tagged fusion. Taking the Carpp *et al.* (2014) data, we selected proteins with light/heavy ratios of at least 5.0, proteins that appeared in all independent NS5 experiments and proteins that were found in GFP control pulldowns not more than two times, generating a list of 73 candidates against our 97. Here, no overlap in datasets was found (Fisher's exact test; P value=0.70). On the other hand, the overlap between our data and that in Germain *et al.* (2014) using N-terminal FLAG-tagged NS5B in distantly related HCV was far more significant (P value= 7.2×10^{-9}), underlining the importance of tag size. While our list was enriched in cytosolic proteins, Carpp *et al.* (2014) showed enrichment in nuclear import and transport system proteins. While DENV-2 NS5 does localize to the nucleus, mutations that eliminate this localization showed little effect on viral replication, casting doubt on the notion of critical interactions with nuclear proteins (Hannemann *et al.*, 2013). It is also possible that ectopic expression of an extra 28 kDa GFP tag could alter protein folding in cells. We have shown that even a short hexahistidine tag at either N- or C-termini of DENV RdRp markedly impaired the polymerase activity (Kamkaew & Chimnaronk, 2015).

In conclusion, we highlighted stringent criteria for effective design of protein tagging, and provided proof-of-concept evidence by generation of viable tagged recombinant DENV-2 possessing an internal TAP tag in NS5. Utilizing our tagged DENV, we revealed here a high-confidence protein interaction network with NS5 in infected human hepatic cells, in which RNP and fatty acid biosynthesis complexes were recruited into DENV replicase. This work provides a general method for tagging of viral proteins and a standard for future studies of virus–host interactions.

METHODS

Primary and tertiary structure analyses of NS5. To seek candidate tag insertion sites with minimal conservation, ten flaviviral NS5-containing polyprotein sequences were aligned using ClustalW2, representing DENV-1 (NCBI accession AHG23185), DENV-2 (AHG23127), DENV-3 (ABG73588.1), DENV-4 (AIG60035.1), West Nile virus (AAT02759.1), Japanese encephalitis virus (AAD20233), yellow fever virus (AAC35903), St. Louis encephalitis virus (AEN02430), Omsk haemorrhagic fever virus (AAR98531) and tick-borne encephalitis virus (ACL97686.1). The alignment results generated integer conservation values for each residue position (Thompson *et al.*, 1994), and subsequently, the means of the data were taken over all 31 residue windows, clarifying regions of particularly high and low conservation.

Following identification of potential conservation-based insertion sites, the available crystal structure of DENV-3 NS5 (PDB ID: 4V0R) was examined to screen out candidates that would be located in structured or hydrophobic regions. Finally, short sequences that various tags would straddle were interrogated against the ELM database (<http://elm.eu.org/>) to reduce the chances that critical linear motifs would be interrupted. Only two internal NS5 locations fulfilled all the above criteria, and were selected for tag insertion.

Insertion of the TAP tag sequences into NS5 of a DENV-2 16681 clone. The cDNA from DENV serotype 2 strain 16681 in the pD2-IC plasmid was used as the template for the insertion of the epitope tag (Kinney *et al.*, 1997). In this work, the TAP tag comprised an octahistidine (His₈) tag, a tri-glycine spacer and FLAG sequence (DYKDDDDK) which was inserted into the NS5 gene in pD2-IC via a standard QuikChange procedure. Briefly, the tag sequences in the forward and reverse primers overlapped by at least 20 nt (Table S1, available in the online Supplementary Material), while the 3' portions of the primers were required to overlap the DENV genome with an annealing temperature of not less than 70 °C. Reactions were conducted in 20 µl volumes with 0.4 U Phusion polymerase (NEB) and not more than 10 ng of template. Twenty-two PCR cycles were performed, with a 10 s denaturation period at 98 °C, a 30 s annealing period at 55 °C and an extension period of 4.5 min at 72 °C. The resulting PCR product was treated with *DpnI* (NEB) prior to bacterial transformation. Colony PCR was used to screen clones for successful mutagenesis, as the tags added 75 nt to the NS5 gene. Positively screened plasmids were sequenced to verify in-frame insertions.

In vitro transcription, transfection and viral titration. DNA templates for *in vitro* run-off transcription were generated by PCR using Phusion polymerase with the forward primer: 5'-GAAATTAATACG-CTCACTATTAGTTGTTAGTCTACGTGGACCGAC-3', carrying a T7 promoter sequence (italics) and the reverse primer: 5'-AGAACC-TGTTGATTCACACAGCACC-3'. The 10.75 kb PCR product was purified with a QIAquick Gel Extraction kit (Qiagen). WT and tagged DENV RNAs were synthesized in a 50 µl reaction with 5 µg purified templates using a RiboMax Large Scale RNA Production kit (Promega) at 37 °C for 4 h. The dsDNA template was removed by DNase I (NEB) treatment, and transcripts were purified via an RNeasy Mini kit (Qiagen). The quality of transcribed RNAs was analysed on denaturing formamide agarose gels.

Ten micrograms of transcribed product was electroporated into 2 × 10⁶ BHK-21 cells following the protocol of Leardkamolkarn *et al.* (2012). Supernatant of transfected cells was collected for foci formation assay at 7 days post-transfection. The supernatant was incubated with BHK-21 cells in 96-well plates for 2 h, and subsequently 200 µl of 1.5 % carboxymethylcellulose and 2 % FBS in Dulbecco's modified Eagle's media (DMEM) was added to cover the cells, and incubated at 37 °C for 3 days. The infected BHK-21 cells were then washed with PBS three times and fixed with 3.7 %

formaldehyde for 10 min at room temperature. The cells were permeabilized by 1 % Triton X-100 in PBS for 10 min and washed with PBS five times. Anti-DENV E protein (Millipore) was diluted 1 : 1000 in PBS supplied with 2 % FBS and 0.05 % Tween-20, and incubated at 37 °C for 2 h. Thereafter, the cells were washed with PBS five times before incubation with goat anti-mouse conjugated HRP antibody at a 1 : 1000 dilution for 45 min at 37 °C. The foci were visualized through SigmaFAST DAP (Sigma) and counted under microscopy.

Cell culture and infection. BHK-21 (baby hamster kidney cells), Huh-7 (human hepatocyte cells), A549 (lung carcinoma cells) and HEK-293 (human embryonic kidney cells) were cultured in DMEM supplemented with 10 % FBS at 37 °C with 5 % CO₂. When the confluences were 75–90 %, the cells were incubated with DENV for 90 min in 2 % FBS DMEM media at 37 °C, 5 % CO₂.

Immunofluorescence assay. At indicated time points, transfected or infected cells were washed with PBS, and then fixed with 3 % paraformaldehyde and 2 % sucrose in PBS. After three washes with PBS, the samples were permeabilized by incubation with Triton X-100 solution (0.5 % Triton X-100, 20 mM HEPES pH 7.8, 50 mM NaCl, 3 mM MgCl₂ and 300 mM sucrose) for 5 min on ice. Cells were washed with PBS four times, and incubated with an anti-NS5 rabbit antibody (Thermo) or an anti-FLAG mouse antibody (Sigma) diluted 1 : 1000 in PBS with 5 % BSA for 2 h at room temperature. Thereafter, the slides were washed three times with PBS, and probed by a goat anti-rabbit conjugated Alexa Fluor 488 (Invitrogen) or goat anti-mouse Alexa Fluor 594 (Jackson ImmunoResearch) antibodies in the dark for 1 h at room temperature before mounting with Prolong Gold Antifade with DAPI (Invitrogen). Protein expression and localization were observed on fluorescence microscopy (Nikon).

Co-immunoprecipitation and immunoblotting. For His tag-affinity purification, infected cells were lysed by incubation with 50 mM HEPES pH 7.2, 150 mM KCl, 25 mM imidazole, 1 % NP-40, 10 % glycerol, 5 mM β-mercaptoethanol (2-ME), 1 × EDTA-free protease inhibitor (GE Healthcare), 1 % Triton X-100, 1 × Phosphatase Inhibitor (Thermo) and 7 U ml⁻¹ DNase (NEB) for 30 min on ice. Cell lysate was cleared via centrifugation at 15 000 r.p.m. for 15 min, and the supernatant was applied to Ni-NTA agarose beads (Qiagen) pre-equilibrated with Ni wash buffer (50 mM HEPES pH 7.2, 150 mM KCl, 25 mM imidazole, 1 % NP-40, 10 % glycerol, 5 mM 2-ME and 1 × EDTA-free protease inhibitor). A 10 µl bed volume of beads was suitable for approximately 10⁷ cells. The resin was gently agitated at 4 °C for 1 h for binding. Unbound materials were removed by at least six cycles of 5 min washing at 4 °C. Elution proceeded with four cycles of treatment with 100 µl elution buffer. In cases where subsequent FLAG purification was not desired, elution buffer was the wash buffer supplied with a final 250 mM imidazole concentration. Otherwise, the elution buffer omitted 2-ME and NP-40, as these components could interfere with FLAG purification.

For the FLAG pull down, infected cells were carefully washed with PBS, and cell pellets were incubated with 2 mM dimethyl pimelimidate at room temperature for 20 min to cross-link protein–protein complexes. Cells were lysed with CLB buffer (50 mM Tris/HCl pH 7.4, 250 mM NaCl, 0.5 % NP-40, 1 mM glycerophosphate, 1 mM sodium orthovanadate and 5 mM EDTA). The total cell lysates were pre-cleared with protein G agarose (Roche) to reduce non-specific binding for 60 min at 4 °C, and subsequently gently mixed with EZview Red Anti-FLAG M2 affinity gels (Sigma) for 4 h at 4 °C. After washing three times with 50 mM Tris/HCl pH 7.4 and 150 mM NaCl, bound proteins were eluted with 30 µl of 1 M glycine pH 2.5 three times. The samples were neutralized by adding 10 µl 1 M Tris/HCl pH 8.0, and concentrated using 10 kDa-cut-off Amicon Ultra filters (Millipore).

Total cell lysates and pulled-down fractions were analysed with 10 % SDS-PAGE, and transferred onto a PVDF membrane. The membranes were blocked with 5 % skim milk in 0.01 % Tween-20, 10 mM Tris/HCl pH 8.0 and 150 mM NaCl (TBST buffer). The membranes were incubated with primary antibody for 12–16 h at 4 °C, washed three times at room temperature with TBST, and probed with a goat anti-rabbit (Thermo) or goat anti-mouse (Novagen) conjugated HRP antibodies for 2 h. The protein bands were detected via chemiluminescence according to the manufacturer's instructions (ECL, GE Healthcare Life Sciences).

Flow cytometry. Cells were collected by centrifugation at 1800 g after treatment with 0.25 % trypsin-EDTA for 3–5 min. The cell pellets were fixed with 3.7 % formaldehyde in PBS for 15 min, and permeabilized with FACS solution containing 0.5 % saponin, 2 % FBS, 2 mM EDTA and 0.05 % AB human serum in PBS for 20 min at room temperature. The DENV E protein was probed by a mouse anti-E primary antibody and a goat anti-mouse FITC-labelled secondary antibody (Dako) for 60 min at 4 °C. Then cells were washed three times with FACS solution, and fixed with 1 % formaldehyde in PBS before analysing with a FACS Caliber (BD). The percentage of DENV-infected cells was calculated using Flowing Software version 2.5.1.

Mass spectrometry. Concentrated samples from FLAG IP were separated on a 10 % SDS-PAGE, and in-gel trypsin digestion was performed as follows. Small gel slices were washed with 25 mM ammoniumbicarbonate (Ambic) in 50 % acetonitrile (ACN) two times. Dehydration proceeded with 100 % ACN two or three times until gel pieces were white, followed by speed vacuum treatment to evaporate the solution. A reducing step was performed by adding 10 mM DTT and 25 mM Ambic and incubating at 56 °C for 45 min. The supernatant was then removed, and gel pieces were incubated with 55 mM iodoacetamine and 25 mM Ambic in the dark for 30 min at room temperature. After washing with 25 mM Ambic for 10 min followed by 100 % ACN, gel pieces were dried by speed-vac for 15 min. Proteins were digested by incubation with 12.5 ng μl^{-1} trypsin (Promega) for 1 h on ice, and processed at 37 °C in 25 mM Ambic overnight. Tryptic peptides were extracted with 50 % ACN two or three times and concentrated via a vacuum centrifuge. Peptide pools were desalted with an octadecyl C_{18} resin before injection into a tandem mass spectrometer (Q-Exactive Plus, Thermo).

Data analysis. Mass spectrometry results were analysed using the X! Tandem algorithm in the Global Proteome Machine software (Craig *et al.*, 2004) and the SEQUEST algorithm in the Proteome Discoverer (PD) software (Thermo). Ensembl and UniProt databases were used in these software packages, respectively. Precursor and fragment mass errors were set to 10 p.p.m. NS5 protein partners were included in the list using a false discovery rate of lower than 1 % as a cut-off based on target-decoy analysis. Only proteins identified by both software approaches were included in the final list of potential NS5 interactors. For the label-free quantification, the list of peptides from PD was further subjected to analysis by Skyline software (MacLean *et al.*, 2010). For Skyline, isotope dot product, a measure that compares apparent isotope ratios in experimental peptides with naturally occurring expected ratios, was used to exclude peptides with isotope dot product value of less than 0.8. The NS5-interacting network was generated using the STRING 10.0 database, with co-occurrence, database and text mining excluded from analysis (Szklarczyk *et al.*, 2015). This network was used as a template to construct a refined network that indicated the number of peptide fragments weighted against molecular mass for all nodes, and also indicated the confidence of STRING interactions at levels 0.9, 0.7 and 0.4 as edge widths. DAVID (Huang *et al.*, 2009a, b) was used for gene-ontology analysis.

ACKNOWLEDGEMENTS

This work was supported by Grants-in-Aid for scientific research from Mahidol University (Thailand) and by the Mid-Career Grant from Thailand Research Fund (TRF) (RSA5680054) to S. C.; S. J. was supported by the Chalmersphrakiat Grant, Faculty of Medicine, Siriraj Hospital, Mahidol University. S. J. and S. C. were also supported by the Advanced Research on Pharmacology Fund, Siriraj Foundation (D003421). This work was also funded by the Office of the Higher Education Commission and Mahidol University under the National Research Universities initiative (NRU), and the DENFREE project (The European Union Seventh Framework Programme, FP7/2007/2011 under Grant Agreement no. 282 378) to A. S. and P. M. T. Pisitkun was supported by Chulalongkorn Academic Advancement into its 2nd Century Project (CUAASC) grant. T. Poyomtip was supported by a scholarship from Science Achievement Scholarship of Thailand (SAST). We thank Poorichaya Somporn for helping in all aspects of mass spectrometry, and Vijitra Learkamolarn for kindly providing the pD2-IC plasmid.

REFERENCES

- Anwar, A., Leong, K. M., Ng, M. L., Chu, J. J. & Garcia-Blanco, M. A. (2009). The polypyrimidine tract-binding protein is required for efficient dengue virus propagation and associates with the viral replication machinery. *J Biol Chem* **284**, 17021–17029.
- Ashour, J., Laurent-Rolle, M., Shi, P. Y. & Garcia-Sastre, A. (2009). NS5 of dengue virus mediates STAT2 binding and degradation. *J Virol* **83**, 5408–5418.
- Aye, K. S., Charngkaew, K., Win, N., Wai, K. Z., Moe, K., Punyadee, N., Thiemmecca, S., Suttitheptumrong, A., Sukpanichnant, S. & other authors (2014). Pathologic highlights of dengue hemorrhagic fever in 13 autopsy cases from Myanmar. *Hum Pathol* **45**, 1221–1233.
- Bhatt, S., Gething, P. W., Brady, O. J., Messina, J. P., Farlow, A. W., Moyes, C. L., Drake, J. M., Brownstein, J. S., Hoen, A. G. & other authors (2013). The global distribution and burden of dengue. *Nature* **496**, 504–507.
- Bidet, K. & Garcia-Blanco, M. A. (2014). Flaviviral RNAs: weapons and targets in the war between virus and host. *Biochem J* **462**, 215–230.
- Brunak, S., Engelbrecht, J. & Knudsen, S. (1991). Prediction of human mRNA donor and acceptor sites from the DNA sequence. *J Mol Biol* **220**, 49–65.
- Brunetti, J. E., Scolaro, L. A. & Castilla, V. (2015). The heterogeneous nuclear ribonucleoprotein K (hnRNP K) is a host factor required for dengue virus and Junin virus multiplication. *Virus Res* **203**, 84–91.
- Carp, L. N., Rogers, R. S., Moritz, R. L. & Aitchison, J. D. (2014). Quantitative proteomic analysis of host-virus interactions reveals a role for Golgi brefeldin A resistance factor 1 (GBF1) in dengue infection. *Mol Cell Proteomics* **13**, 2836–2854.
- Chiu, H. C., Hannemann, H., Heesom, K. J., Matthews, D. A. & Davidson, A. D. (2014). High-throughput quantitative proteomic analysis of dengue virus type 2 infected A549 cells. *PLoS One* **9**, e93305.
- Craig, R., Cortens, J. P. & Beavis, R. C. (2004). Open source system for analyzing, validating, and storing protein identification data. *J Proteome Res* **3**, 1234–1242.
- Cristea, I. M., Rozjabek, H., Molloy, K. R., Karki, S., White, L. L., Rice, C. M., Rout, M. P., Chait, B. T. & MacDonald, M. R. (2010). Host factors associated with the Sindbis virus RNA-dependent RNA polymerase: role for G3BP1 and G3BP2 in virus replication. *J Virol* **84**, 6720–6732.

- Dinkel, H., Michael, S., Weatheritt, R. J., Davey, N. E., Van Roey, K., Altenberg, B., Toedt, G., Uyar, B., Seiler, M. & other authors (2012). ELM—the database of eukaryotic linear motifs. *Nucleic Acids Res* 40 (D1), D242–D251.
- Dong, H., Zhang, B. & Shi, P. Y. (2008). Flavivirus methyltransferase: a novel antiviral target. *Antiviral Res* 80, 1–10.
- Dong, H., Fink, K., Züst, R., Lim, S. P., Qin, C. F. & Shi, P. Y. (2014). Flavivirus RNA methylation. *J Gen Virol* 95, 763–778.
- Doolittle, J. M. & Gomez, S. M. (2011). Mapping protein interactions between Dengue virus and its human and insect hosts. *PLoS Negl Trop Dis* 5, e954.
- Duangchinda, T., Dejnirattisai, W., Vasanawathana, S., Limpitikul, W., Tangthawornchaikul, N., Malasit, P., Mongkolsapaya, J. & Screaton, G. (2010). Immunodominant T-cell responses to dengue virus NS3 are associated with DHF. *Proc Natl Acad Sci U S A* 107, 16922–16927.
- Fink, J., Gu, F., Ling, L., Tolfvenstam, T., Olfat, F., Chin, K. C., Aw, P., George, J., Kuznetsov, V. A. & other authors (2007). Host gene expression profiling of dengue virus infection in cell lines and patients. *PLoS Negl Trop Dis* 1, e86.
- Germain, M. A., Chatel-Chaix, L., Gagné, B., Bonneil, É., Thibault, P., Pradezynski, F., de Chasse, B., Meyniel-Schicklin, L., Lotteau, V. & other authors (2014). Elucidating novel hepatitis C virus-host interactions using combined mass spectrometry and functional genomics approaches. *Mol Cell Proteomics* 13, 184–203.
- Hannemann, H., Sung, P. Y., Chiu, H. C., Yousuf, A., Bird, J., Lim, S. P. & Davidson, A. D. (2013). Serotype-specific differences in dengue virus non-structural protein 5 nuclear localization. *J Biol Chem* 288, 22621–22635.
- Heaton, N. S., Perera, R., Berger, K. L., Khadka, S., Lacount, D. J., Kuhn, R. J. & Randall, G. (2010). Dengue virus nonstructural protein 3 redistributes fatty acid synthase to sites of viral replication and increases cellular fatty acid synthesis. *Proc Natl Acad Sci U S A* 107, 17345–17350.
- Higa, L. M., Caruso, M. B., Canellas, F., Soares, M. R., Oliveira-Carvalho, A. L., Chapeaurouge, D. A., Almeida, P. M., Perales, J., Zingali, R. B. & Da Poian, A. T. (2008). Secretome of HepG2 cells infected with dengue virus: implications for pathogenesis. *Biochim Biophys Acta* 1784, 1607–1616.
- Huang, W., Sherman, B. T. & Lempicki, R. A. (2009a). Bioinformatics enrichment tools: paths toward the comprehensive functional analysis of large gene lists. *Nucleic Acids Res* 37, 1–13.
- Huang, W., Sherman, B. T. & Lempicki, R. A. (2009b). Systematic and integrative analysis of large gene lists using DAVID bioinformatics resources. *Nat Protoc* 4, 44–57.
- Jiang, L., Yao, H., Duan, X., Lu, X. & Liu, Y. (2009). Polypyrimidine tract-binding protein influences negative strand RNA synthesis of dengue virus. *Biochem Biophys Res Commun* 385, 187–192.
- Kamkaew, M. & Chimnarong, S. (2015). Characterization of soluble RNA-dependent RNA polymerase from dengue virus serotype 2: The polyhistidine tag compromises the polymerase activity. *Protein Expr Purif* 112, 43–49.
- Kawamura-Nagaya, K., Ishibashi, K., Huang, Y. P., Miyashita, S. & Ishikawa, M. (2014). Replication protein of tobacco mosaic virus cotranslationally binds the 5' untranslated region of genomic RNA to enable viral replication. *Proc Natl Acad Sci U S A* 111, E1620–E1628.
- Khadka, S., Vangeloff, A. D., Zhang, C., Siddavatam, P., Heaton, N. S., Wang, L., Sengupta, R., Sahasrabudhe, S., Randall, G. & other authors (2011). A physical interaction network of dengue virus and human proteins. *Mol Cell Proteomics* 10, 012187.
- Khromykh, A. A., Sedlak, P. L., Guyatt, K. J., Hall, R. A. & Westaway, E. G. (1999). Efficient trans-complementation of the flavivirus kunjin NS5 protein but not of the NS1 protein requires its coexpression with other components of the viral replicase. *J Virol* 73, 10272–10280.
- Kinney, R. M., Butrapet, S., Chang, G. J., Tsuchiya, K. R., Roehrig, J. T., Bhamarapravati, N. & Gubler, D. J. (1997). Construction of infectious cDNA clones for dengue 2 virus: strain 16681 and its attenuated vaccine derivative, strain PDK-53. *Virology* 230, 300–308.
- Krishnan, M. N. & Garcia-Blanco, M. A. (2014). Targeting host factors to treat West Nile and dengue viral infections. *Viruses* 6, 683–708.
- Le Breton, M., Meyniel-Schicklin, L., Deloire, A., Coutard, B., Canard, B., de Lamballerie, X., Andre, P., Rabourdin-Combe, C., Lotteau, V. & Davoust, N. (2011). Flavivirus NS3 and NS5 proteins interaction network: a high-throughput yeast two-hybrid screen. *BMC Microbiol* 11, 234.
- Leardkamolkarn, V., Sirigulpanit, W., Chotiwan, N., Kumkate, S. & Huang, C. Y. (2012). Development of Dengue type-2 virus replicons expressing GFP reporter gene in study of viral RNA replication. *Virus Res* 163, 552–562.
- Li, P., Bai, X., Cao, Y., Han, C., Lu, Z., Sun, P., Yin, H. & Liu, Z. (2012). Expression and stability of foreign epitopes introduced into 3A nonstructural protein of foot-and-mouth disease virus. *PLoS One* 7, e41486.
- Liew, K. J. & Chow, V. T. (2006). Microarray and real-time RT-PCR analyses of a novel set of differentially expressed human genes in ECV304 endothelial-like cells infected with dengue virus type 2. *J Virol Methods* 131, 47–57.
- Liu, W. J., Sedlak, P. L., Kondratieva, N. & Khromykh, A. A. (2002). Complementation analysis of the flavivirus Kunjin NS3 and NS5 proteins defines the minimal regions essential for formation of a replication complex and shows a requirement of NS3 in cis for virus assembly. *J Virol* 76, 10766–10775.
- MacLean, B., Tomazela, D. M., Shulman, N., Chambers, M., Finney, G. L., Frewen, B., Kern, R., Tabb, D. L., Liebler, D. C. & MacCoss, M. J. (2010). Skyline: an open source document editor for creating and analyzing targeted proteomics experiments. *Bioinformatics* 26, 966–968.
- Mairiang, D., Zhang, H., Sodja, A., Murali, T., Suriyaphol, P., Malasit, P., Limjindaporn, T. & Finley, R. L. Jr. (2013). Identification of new protein interactions between dengue fever virus and its hosts, human and mosquito. *PLoS One* 8, e53535.
- Pando-Robles, V., Osés-Prieto, J. A., Rodríguez-Gandarilla, M., Meneses-Romero, E., Burlingame, A. L. & Batista, C. V. (2014). Quantitative proteomic analysis of Huh-7 cells infected with Dengue virus by label-free LC-MS. *J Proteomics* 111, 16–29.
- Póvoa, T. F., Alves, A. M., Oliveira, C. A., Nuovo, G. J., Chagas, V. L. & Paes, M. V. (2014). The pathology of severe dengue in multiple organs of human fatal cases: histopathology, ultrastructure and virus replication. *PLoS One* 9, e83386.
- Rigaut, G., Shevchenko, A., Rutz, B., Wilm, M., Mann, M. & Séraphin, B. (1999). A generic protein purification method for protein complex characterization and proteome exploration. *Nat Biotechnol* 17, 1030–1032.
- Sabourin, M., Tuzon, C. T., Fisher, T. S. & Zakian, V. A. (2007). A flexible protein linker improves the function of epitope-tagged proteins in *Saccharomyces cerevisiae*. *Yeast* 24, 39–45.
- Schoggins, J. W., Dorner, M., Feulner, M., Imanaka, N., Murphy, M. Y., Ploss, A. & Rice, C. M. (2012). Dengue reporter viruses reveal viral dynamics in interferon receptor-deficient mice and sensitivity to interferon effectors in vitro. *Proc Natl Acad Sci U S A* 109, 14610–14615.

- Szklarczyk, D., Franceschini, A., Wyder, S., Forslund, K., Heller, D., Huerta-Cepas, J., Simonovic, M., Roth, A., Santos, A. & other authors (2015). STRING v10: protein-protein interaction networks, integrated over the tree of life. *Nucleic Acids Res* **43** (D1), D447–D452.
- Teterina, N. L., Lauber, C., Jensen, K. S., Levenson, E. A., Gorbalenya, A. E. & Ehrenfeld, E. (2011). Identification of tolerated insertion sites in poliovirus non-structural proteins. *Virology* **409**, 1–11.
- Thompson, J. D., Higgins, D. G. & Gibson, T. J. (1994). CLUSTAL W: improving the sensitivity of progressive multiple sequence alignment through sequence weighting, position-specific gap penalties and weight matrix choice. *Nucleic Acids Res* **22**, 4673–4680.
- Uchil, P. D., Kumar, A. V. & Satchidanandam, V. (2006). Nuclear localization of flavivirus RNA synthesis in infected cells. *J Virol* **80**, 5451–5464.
- Usme-Ciro, J. A., Lopera, J. A., Enjuanes, L., Almazán, F. & Gallego-Gomez, J. C. (2014). Development of a novel DNA-launched dengue virus type 2 infectious clone assembled in a bacterial artificial chromosome. *Virus Res* **180**, 12–22.
- Vandergaast, R., Hoover, L. I., Zheng, K. & Fredericksen, B. L. (2014). Generation of West Nile virus infectious clones containing amino acid insertions between capsid and capsid anchor. *Viruses* **6**, 1637–1653.
- Wang, M., Herrmann, C. J., Simonovic, M., Szklarczyk, D. & von Mering, C. (2015). Version 4.0 of PaxDb: protein abundance data, integrated across model organisms, tissues, and cell-lines. *Proteomics* **15**, 3163–3168.
- Welsch, S., Miller, S., Romero-Brey, I., Merz, A., Bleck, C. K., Walther, P., Fuller, S. D., Antony, C., Krijnse-Locker, J. & Bartenschlager, R. (2009). Composition and three-dimensional architecture of the dengue virus replication and assembly sites. *Cell Host Microbe* **5**, 365–375.
- WHO (2009). *Dengue: Guidelines for Diagnosis, Treatment, Prevention and Control: New Edition*. Geneva: World Health Organization.
- Xu, S., Pei, R., Guo, M., Han, Q., Lai, J., Wang, Y., Wu, C., Zhou, Y., Lu, M. & Chen, X. (2012). Cytosolic phospholipase A2 gamma is involved in hepatitis C virus replication and assembly. *J Virol* **86**, 13025–13037.
- Zou, G., Xu, H. Y., Qing, M., Wang, Q. Y. & Shi, P. Y. (2011). Development and characterization of a stable luciferase dengue virus for high-throughput screening. *Antiviral Res* **91**, 11–19.